BIOCHEMISTRY
including biophysical chemistry & molecular biology

Article

pubs.acs.org/biochemistry

Leishmania major Peroxidase Is a Cytochrome *c* Peroxidase

Victoria S. Jasion and Thomas L. Poulos*

Departments of Molecular Biology and Biochemistry, Chemistry, and Pharmaceutical Sciences, University of California, Irvine, California 92697-3900, United States

ABSTRACT: *Leishmania major* peroxidase (LmP) exhibits both ascorbate and cytochrome *c* peroxidase activities. Our previous results illustrated that LmP has a much higher activity against horse heart cytochrome *c* than ascorbate, suggesting that cytochrome *c* may be the biologically important substrate. To elucidate the biological function of LmP, we have recombinantly expressed, purified, and determined the 2.08 Å crystal structure of *L. major* cytochrome *c* (LmCytc). Like other types of cytochrome *c*, LmCytc has an electropositive surface surrounding the exposed heme edge that serves as the site of docking with redox partners. Kinetic assays performed with LmCytc and LmP show that LmCytc is a much better substrate for LmP than horse heart cytochrome *c*. Furthermore, unlike the well-studied yeast system, the reaction follows classic Michaelis−Menten kinetics and is sensitive to an increasing ionic strength. Using the yeast cocrystal as a control, protein−protein docking was performed using Rosetta to develop a model for the binding of LmP and LmCytc. These results suggest that the biological function of LmP is to act as a cytochrome *c* peroxidase.

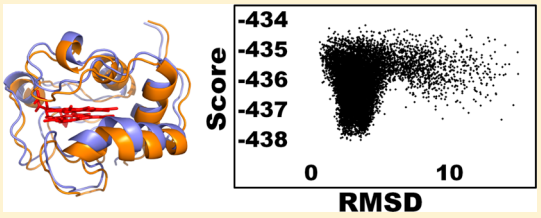

Saccharomyces cerevisiae cytochrome *c* peroxidase (CCP) has long served as a paradigm for interprotein electron transfer.[1] CCP and other heme peroxidases form distinct spectroscopically well-defined intermediates called Compounds I and II in the following reaction cycle.

$$\mathrm{Fe(III)R + H_2O_2 \rightarrow \underset{\text{Compound I}}{Fe(IV){-}OR^{\bullet+}} + H_2O} \quad (1)$$

$$\mathrm{Fe(IV){-}OR^{\bullet+} + S \rightarrow \underset{\text{Compound II}}{Fe(IV){-}OR} + S^{\bullet}} \quad (2)$$

$$\mathrm{Fe(IV){-}OR + S \rightarrow Fe(III)R + H_2O + S^{\bullet}} \quad (3)$$

The intermediate Compound I forms once H_2O_2 is heterolytically cleaved, releasing a water molecule. The remaining O atom oxidizes the heme iron to Fe(IV) and an organic moiety, R, to a cation radical. For most heme peroxidases, R is the porphyrin ring.[2] Upon two electron transfer events from two substrate molecules, S, the enzyme returns to the resting state with water occupying the active site. The types of substrates oxidized by various peroxidases include ascorbate, lignin, manganese, and a variety of small aromatic organic molecules. CCP, however, uses another protein, cytochrome *c*, as its substrate. Moreover, CCP forms a unique Compound I radical on Trp191 that is adjacent to the proximal His ligand.[3]

Not surprisingly, yeast is not unique in having a CCP, but to date, only one other CCP-like peroxidase, *Leishmania major* peroxidase (LmP), has been well characterized.[4−6] Trp208 in LmP is analogous to Trp191 in CCP, and Yadav et al.[6] showed that the Trp208Phe mutant exhibits dramatically decreased activity. We recently determined the crystal structure of LmP and found, using mutagenesis and electron paramagnetic resonance spectroscopy, that Trp208 does form a stable radical as does Trp191 in yeast CCP and that, like CCP, the local electrostatic environment stabilizes the cationic Trp208 radical.[7−12]

Although LmP was initially characterized as a dual peroxidase with both ascorbate and cytochrome *c* peroxidase activities,[4] the close similarity to yeast CCP and the location of LmP in *L. major* mitochondria[13] strongly suggest that the biological substrate for LmP is Cytc. Moreover, our highly purified LmP used for crystallization exhibits good activity toward horse heart Cytc, although the activity is still well below that of yeast CCP. As one might expect, yeast Cytc is a better substrate for yeast CCP than other Cytcs, and we can anticipate that *L. major* Cytc should be a better substrate for LmP. We therefore have purified and determined the crystal structure of *L. major* Cytc (LmCytc), characterized the reaction between LmP and LmCytc, and developed a model of the LmP−LmCytc complex.

EXPERIMENTAL PROCEDURES

Cloning. The sequence of cytochrome *c* from *L. major* (strain Friedlin) was obtained from GenBank.[14] LmCytc was synthesized by GenScript, with optimized codons for *Escherichia coli* expression, into the construct pBPCYC1, replacing yeast cytochrome *c*.[15]

Protein Expression and Purification. The LmCytc plasmid was transformed into *E. coli* BL21(DE3) cells and plated onto LB agar with ampicillin (100 μg/mL). One colony was picked and grown in LB Miller and ampicillin (100 μg/mL) overnight at 37 °C with 220 rpm agitation. Expression cultures of TB medium with ampicillin (100 μg/mL) were

Received: February 6, 2012
Revised: February 28, 2012
Published: February 29, 2012

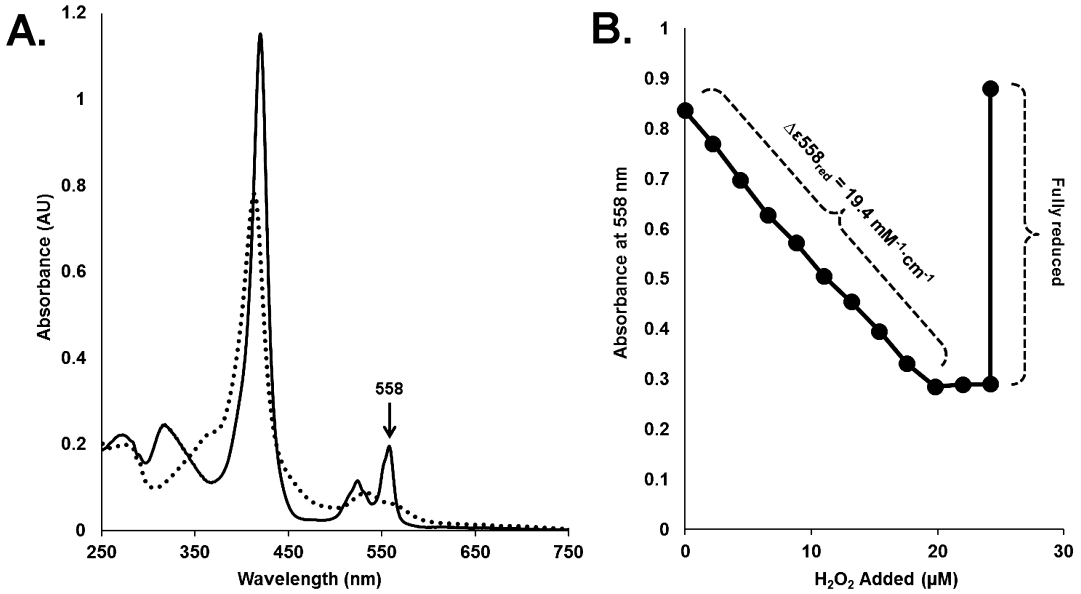

Figure 1. (A) Oxidized (···) and reduced (—) UV−vis spectra of LmCytc. The maximum used to follow oxidation of reduced LmCytc by LmP is at 558 nm. (B) Enzymatic determination of $\Delta\varepsilon_{558red}$. Aliquots of 2.2 μM H_2O_2 were added until LmCytc could no longer be oxidized by LmP. The ε_{558} of the enzymatically oxidized sample was determined to be 9.6 mM^{-1} cm^{-1}, so that $\Delta\varepsilon_{558red}$ was calculated to be 19.4 mM^{-1} cm^{-1}. The sample was then fully reduced by addition of granules of sodium dithionite.

inoculated with the overnight culture (1:100). The cells were grown at 37 °C with 220 rpm agitation in a New Brunswick Scientific C25KC incubator. After 24 h, cells were harvested by centrifugation and stored at −80 °C. Cells were thawed overnight at 4 °C and resuspended by being stirred for 1 h at 4 °C in 500 mM potassium phosphate (pH 6.4), 0.5 mM PMSF, 2 mM $MgCl_2$, 100 μg/mL lysozyme, 0.2 μg/mL DNase, and 0.2 μg/mL leupeptin. Sonication on ice for 5 min at intervals of 1 min (sonicate for 1 min and rest for 1 min) ensured efficient lysis. The soluble fraction was isolated by centrifugation at 37500*g* and 4 °C for 1 h. The lysate (~100 mL) was then dialyzed against 4 L of 10 mM potassium phosphate (pH 6.4) for 4 h at 4 °C and placed into fresh buffer for an overnight dialysis at 4 °C. Precipitated proteins were then separated from the lysate by centrifugation at 10800*g* and 4 °C for 30 min. The supernatant was pooled, and the heme iron was oxidized with ~70 mg of potassium ferricyanide. The ionic strength was reduced to 5 mM by addition of autoclaved water. The lysate was then loaded onto a 25 mL CM Sepharose gravity column that had been pre-equilibrated with 10 mM sodium phosphate (pH 6.4) at a rate of 3 mL/min and 4 °C. The column was washed with 20 column volumes (CV) of 10 mM potassium phosphate (pH 6.4). The protein was eluted with a gradient from 10 to 250 mM potassium phosphate (pH 6.4). The fractions with R_z (A_{414}/A_{280}) values between 3.2 and 4.5 were pooled and loaded onto a Superdex 75 26/60 column that had been pre-equilibrated with 50 mM potassium phosphate (pH 7.0) and 5% glycerol at a flow rate of 0.5 mL/min and 4 °C. The resulting fractions were analyzed by 15% sodium dodecyl sulfate−polyacrylamide gel electrophoresis, and the most pure fractions were pooled. The resulting sample had an R_z (A_{414}/A_{280}) value of 4.2. The protein concentration of LmCytc was calculated with the molar extinction coefficient (ε_{280} = 27.1 mM^{-1} cm^{-1}) determined using the Pierce Modified Lowry Protein Assay Kit with horse heart cytochrome *c* (Sigma-Aldrich) used as the sample for the standard curve. The heme content of LmCytc was 97%, as determined with the hemochromagen assay used previously.[12,16] It is worth mentioning that LmCytc has a nonstandard *c*-type heme group because it conserves only one Cys residue and can form only one thioether linkage between the heme vinyl group and Cys. This resulted in a different spectrum for the hemochromagen assay, and the maximum used to calculate the LmCytc heme content was at 552 nm as opposed to 550 nm, which is the value for horse heart cytochrome *c* or any standard *c*-type heme groups.[16,17] The Soret molar extinction coefficient of oxidized LmCytc was determined to be ε_{414} = 115.6 mM^{-1} cm^{-1}. The molar extinction coefficient of reduced LmCytc (ε_{558red}) was determined to be 29 mM^{-1} cm^{-1} by complete reduction of LmCytc with excess sodium dithionite. LmP was expressed and purified as previously described.[12]

Enzymatic Determination of the Reduced LmCytc Extinction Coefficient. The reduced spectrum of LmCytc exhibits a unique maximum at 558 nm (Figure 1A). To ensure this maximum was the best one for use in enzyme kinetics, a simple dithionite titration was first completed by addition of 2 nmol of sodium dithionite to 10.5 nmol of LmCytc (data not shown). As expected, the magnitude of the 558 nm peak increased with an increasing sodium dithionite concentration. The molar extinction coefficient for oxidation of LmCytc ($\Delta\varepsilon_{558}$) was determined enzymatically to be 19.4 mM^{-1} cm^{-1}, using the same protocol used for horse heart and yeast cytochrome *c*.[18] Briefly, in a cuvette containing 30 μM reduced LmCytc and 50 nM LmP, 2.2 μM H_2O_2 was titrated until LmCytc was fully oxidized (Figure 1B).

Steady-State Activity Assays. Spectrophotometric steady-state activity assays using reduced LmCytc were performed at room temperature using a Cary 3E UV−visible spectrophotometer. LmCytc was reduced by adding granules of sodium dithionite and incubated on ice for 30 min. Dithionite was removed by gel filtration over a G10 Sephadex column pre-equilibrated with 50 mM potassium phosphate (pH 7.0). After dithionite had been removed, LmCytc was then concentrated in a 10K molecular weight cutoff centricon at 4 °C so that a

dx.doi.org/10.1021/bi300169x | *Biochemistry* 2012, 51, 2453−2460

smaller volume could be used without altering the reaction conditions in the cuvette. The concentration of reduced LmCytc was determined using the molar extinction coefficient (ε_{558red}) of 29 mM^{-1} cm^{-1}, and the steady-state oxidation of reduced LmCytc was calculated using a $\Delta\varepsilon_{558}$ of 19.4 mM^{-1} cm^{-1}. Over the course of a 4−5 h enzyme assay experiment, approximately 9% of the LmCytc spontaneously oxidized. The LmP concentration was determined using the Soret molar extinction coefficient (ε_{408} = 113.6 mM^{-1} cm^{-1}).[12] Hydrogen peroxide was standardized as outlined by Fowler and Bright.[19] For ionic strength and pH dependencies, LmP was freshly diluted to a working concentration of 5 nM in the appropriate reaction buffer for each condition. The final reaction was conducted in 1 mL of buffer with the following concentrations: 50 pM LmP, 30 μM reduced LmCytc, and 0.180 mM hydrogen peroxide. For the determination of K_M, the assays were completed in 25 mM potassium phosphate (pH 6.5), 50 pM LmP, and 0.180 mM hydrogen peroxide. The reaction was initiated by addition of hydrogen peroxide and monitored for 1 min.

Crystallization of LmCytc. The Pre-Crystallization Test (Hampton) was used to determine the most promising range of protein concentrations, 450 μM, for the initial screenings of LmCytc. Using a high-throughput nanoliter dispensing robot, the Mosquito, an initial crystallization condition was identified: 1.6 M trisodium citrate (pH 6.5) at room temperature. These crystals were long, delicate needle clusters that shattered and disappeared when we made any attempt to harvest them. Various attempts to optimize this condition proved to be unsuccessful. Optimization was completed by changing the buffer from 50 mM potassium phosphate (pH 7.0) to 50 mM potassium phosphate (pH 6.4) and rescreening various commercial crystallization kits. Larger crystal rods were found in 30% PEG 2K MME and 0.1 M potassium bromide using hanging drop vapor diffusion at room temperature. These crystals had a two-dimensional rod morphology and were often not single crystals. Even crystals that appeared to be single resulted in unuseable data sets because of their high mosaicity. Optimizations between 35 and 40% PEG 2K MME and 0.15 and 0.3 M potassium bromide led to one crystal from ∼150 drops with a clear three-dimensional triangular morphology. For cryo, 1 μL of 35% PEG 2K MME, 25 mM potassium phosphate (pH 6.4), 0.17 mM potassium bromide, 5% glycerol, and 2.5% PEG 200 were added to the crystal drop. This mixture was allowed to sit for 5 min, and the crystal was then transferred to washes of the same conditions except with an increasing PEG 200 concentration, from 5% to 10% and finally to 16%.

Structural Determination and Refinement. A 2.08 Å resolution data set was collected using an in-house Rigaku Micromax 007 rotating anode with a Saturn 944 detector, and the crystal belonged to space group $P2_12_12_1$ with one molecule per asymmetric unit. The LmCytc structure was determined by molecular replacement with yeast cytochrome *c* used as the search model (PDB entry 1YCC). Data were indexed, integrated, and scaled using HKL2000.[20] Molecular replacement calculations were conducted with Phaser[21] through the CCP4i graphic interface.[22,23] COOT was used to manually replace the appropriate residues.[24,25] Refinement was completed with phenix refine.[26,27] Coordinate and structure factor files were deposited in the Protein Data Bank (entry 4DY9). Crystallographic data collection and refinement statistics are listed in Table 1, where all R_{free} values are calculated with 5% of the data excluded from refinements.

Table 1. Crystallographic Data Collection and Refinement Statistics for LmCytc

space group	$P2_12_12_1$
unit cell dimensions [*a*, *b*, *c* (Å)]	35.280, 44.000, 64.3798
resolution range (Å)	36.3−2.08
radiation source	Rigaku MicroMax-007HF
wavelength (Å)	1.54
total no. of observations	63083
no. of unique reflections (highest shell)	11498 (534)
completeness (%) (highest shell)	99.1 (97.8)
R_{sym} (highest shell)	0.043 (0.068)
$\langle I/\sigma \rangle$ (highest shell)	64.3 (38.6)
Wilson *B* factor	17
no. of reflections used in refinement	6330
resolution range (Å) in refinement	22.0−2.08
R_{work}	0.1611
R_{free}	0.2117
rmsd for bonds (Å)	0.007
rmsd for angles (deg)	1.214

Rosetta Docking. For global docking, LmP and LmCytc were aligned over the yeast cocrystal structure (PDB entry 2PCC) in PyMOL with rmsds of 0.7 and 0.8, respectively.[28] The resulting coordinates were then prepacked using Rosetta 3.2.1 with the following flags: -use_input_sc, -ex1, -ex2aro, -partners A_B (where LmCytc is rotated around LmP), and -unboundrot (where the single unbound coordinates were defined). LmP and LmCytc were then globally docked and locally refined. The heme and cations were included in the prepacking and docking process. The yeast system was prepacked, globally docked, and locally refined in the same manner. The crystal structure of *Equus caballus* (horse heart, hh) cytochrome *c* with yeast CCP (PDB entry 2PCB) was globally docked and locally refined in the same manner as the entire yeast and *L. major* system, except that prepacking resulted in bad contacts so the starting structure was the native crystal structure for each docking attempt. The unbound structures were defined using the following structures: yeast CCP (PDB entry 2CYP), yeast Cytc (PDB entry 1YCC), horse heart (hh) Cytc (PDB entry 1HRC), LmP (PDB entry 3RIV), and LmCtyc (PDB entry 4DY9). The details of the various docking protocols are outlined in Table 2.

RESULTS AND DISCUSSION

Crystal Structure of LmCytc. The structure of LmCytc is very similar to that of yeast Cytc, with an rmsd of 0.70 Å for 94 common Cα atoms, as determined in PyMOL. LmCytc has a unique N-terminal sequence with 10 more residues than horse heart and yeast Cytc, but there is no electron density for the first five residues. LmCytc also differs from most other Cytcs by having only one thioether bond formed between a Cys residue and one heme vinyl group rather than two. This difference probably accounts for the slight spectral differences between LmCytc and yeast Cytc. Most important for docking to redox partners is the distribution of charges surrounding the exposed heme edge. Here LmCytc closely resembles yeast Cytc, showing that those binding interfaces of the Cytcs are highly conserved (Figure 2). However, the binding interfaces of CCP and LmP are noticeably different. For example, Glu290 in CCP

dx.doi.org/10.1021/bi300169x | *Biochemistry* 2012, 51, 2453−2460

Table 2. Rosetta Docking Parameters

system	docking type	flags	no. of structures generated	input structure	plot (Figure 4)	lowest energy	rmsd
2PCC, CCP, Cytc	global	use_input_sc, ex1, ex2aro, unboundrot	1000	prepacked	A	−318.2	10.2
2PCC, CCP, Cytc	local refinement	use_input_sc, ex1, ex2aro, unboundrot, docking_local_refine	1000	prepacked	B	−455.8	4.2
L. major, LmP, LmCytc	global	use_input_sc, ex1, ex2aro, unboundrot	10000	aligned over 2PCC and prepacked	C	−433.9	11.6
L. major, LmP, LmCytc	local refinement	use_input_sc, ex1, ex2aro, unboundrot, docking_local_refine	10000	aligned over 2PCC and prepacked	D	−438.3	2.5

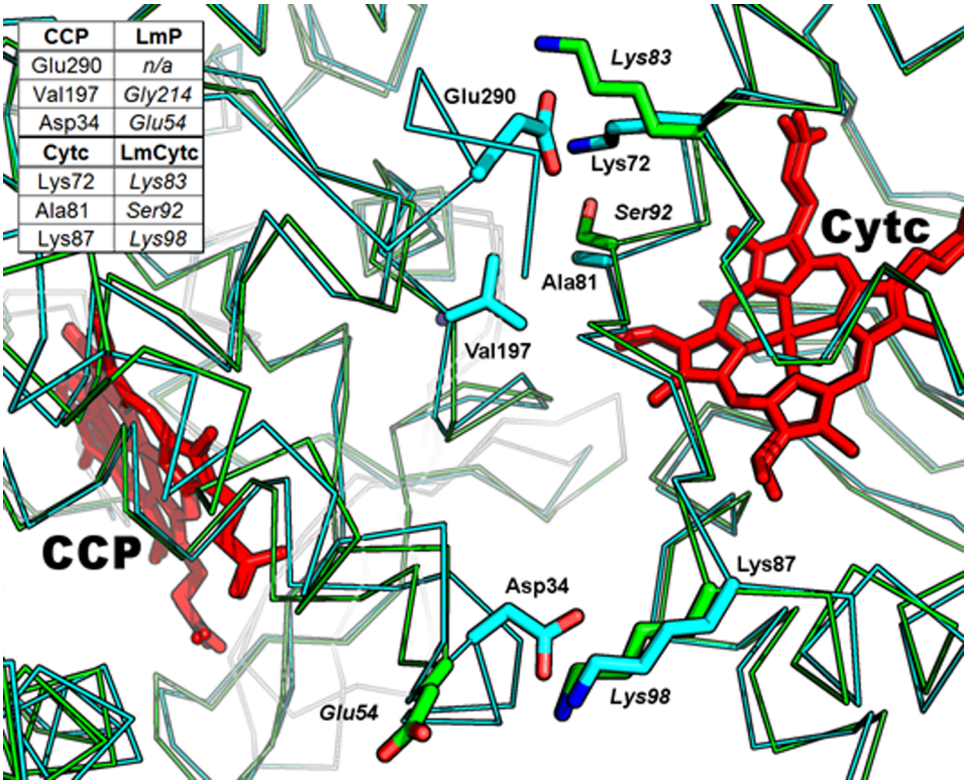

Figure 2. Alignment of LmP and LmCytc (green) over the cocrystal coordinates of the yeast system (PDB entry 2PCC) (cyan). ITC studies illustrated that these residues in the yeast system affect CCP and Cytc complex formation.[33] Italicized labels correspond to the Lm system. This figure and Figures 5 and 7 were generated with PyMOL (Schrödinger, LLC).

is not present in LmP because it lacks this entire C-terminal region. The hydrophobic interaction between Val187 in CCP and Ala81 in Cytc is not present in the Lm system, which has Gly214 and Ser92 at the analogous positions. This indicates that the LmP−LmCytc complex may differ in both structure and dependence on other environmental parameters such as ionic strength. We therefore characterized the steady-state activity of LmP using LmCytc as a substrate.

Steady-State Activity Assays. LmP exhibits a ∼2-fold increase in cytochrome *c* activity with its endogenous substrate, LmCytc, versus previous kinetics with horse heart Cytc.[12] Optimal activity occurs at 25 mM potassium phosphate (pH 6.5) (Figure 3). LmP activity also is very sensitive to ionic strength. Increasing the ionic strength, above 25 mM, results in a steady decrease in activity, and at 200 mM potassium phosphate (pH 6.5), nearly 90% of the activity is lost. This sharply contrasts with the case for yeast CCP, in which the activity increases with an increasing ionic strength up to ∼100 mM and then decreases with an increasing ionic strength.[30] K_M and k_{cat} were determined by using the equation from the best fit line of the Lineweaver−Burk plot (Figure 4). K_M is 6 μM, and the efficiency (k_{cat}/K_M) is 1.6×10^8 M^{-1} s^{-1}, which is on the same order of magnitude as that of the yeast system.[30] LmP also obeys simple Michaelis−Menten kinetics. This is quite different from yeast CCP, for which Eadie−Hofstee plots show a break that has been attributed to a second binding site for Cytc.[30]

The fact that LmCytc is a better substrate than horse heart Cytc can be partially rationalized on the basis of subtle differences between the structures of the various Cytcs. Using the yeast CCP−Cytc complex as a guide,[28] the locations of Lys and Arg residues are the same in Lm, yeast, and horse heart[29] (PDB entry 1HRC) at the binding interface. Toward the periphery of the complex where both yeast and horse heart Cytc have Lys27, LmCytC has Gly38, and where LmCytc has Ser36, horse heart has Lys25 and yeast has Pro25. The main difference directly at the interface is the fact that Ser92 in LmCytc is Ala82 in yeast and Ile81 in horse heart. Therefore, horse heart Cytc has a much bulkier amino acid, Ile versus Ala, at the interface. This may be one reason horse heart Cytc is not as good a substrate as LmCytc.

dx.doi.org/10.1021/bi300169x | *Biochemistry* 2012, 51, 2453−2460

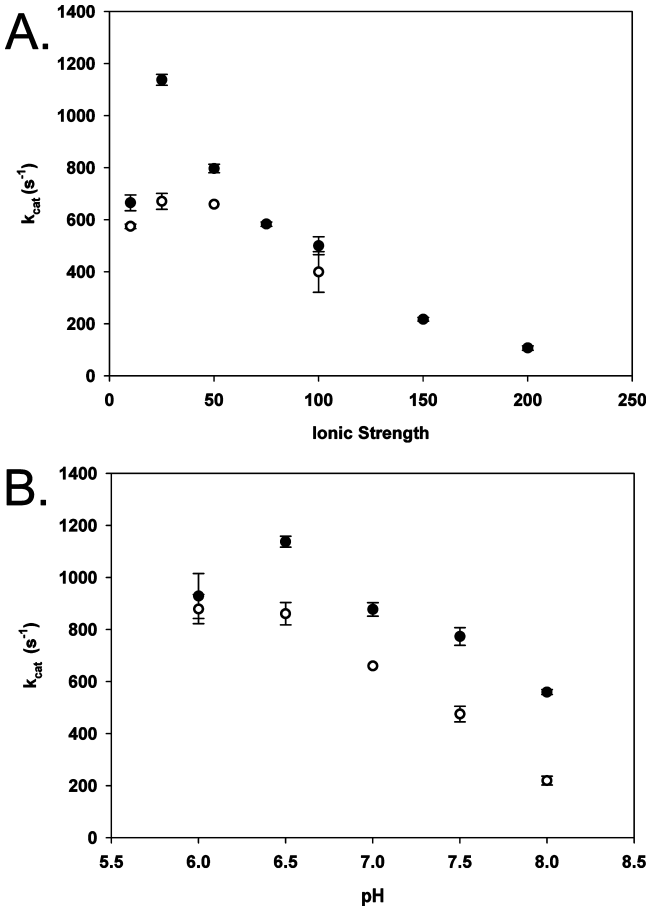

Figure 3. (A) Ionic strength dependency of LmP oxidation of LmCytc. Filled circles represent data for potassium phosphate (pH 6.5) while empty circles data for potassium phosphate (pH 7.0). (B) LmP oxidation of LmCytc vs pH. Filled circles represent data for 25 mM potassium phosphate and empty circles data for 50 mM potassium phosphate. The highest rate of turnover was achieved at 25 mM potassium phosphate (pH 6.5) in both the ionic strength assays and the pH dependence assay.

Computer Docking. The electrostatic surface potential of *S. cerevisiae* CCP and Cytc illustrates why the binding of these partners is electrostatically driven (Figure 5). LmP and LmCytc have the same complementary electrostatic binding surfaces as their yeast counterparts, although they are not as intense. LmP and CCP both have a blanket distribution of negative electrostatic potential on the Cytc binding surface, while both yeast Cytc and LmCytc have strong positive potentials on the corresponding interface. Because LmP and LmCytc are electrostatically so similar to yeast CCP and Cytc, we had high confidence in using the yeast cocrystal coordinates as the template for LmP and LmCytc docking. To develop a model of the LmP–LmCytc complex, we start by simply sumperimposing the two Lm proteins onto their yeast counterparts. The resulting model shows significant steric clashes at the interprotein interface, and simple side chain torsion angle

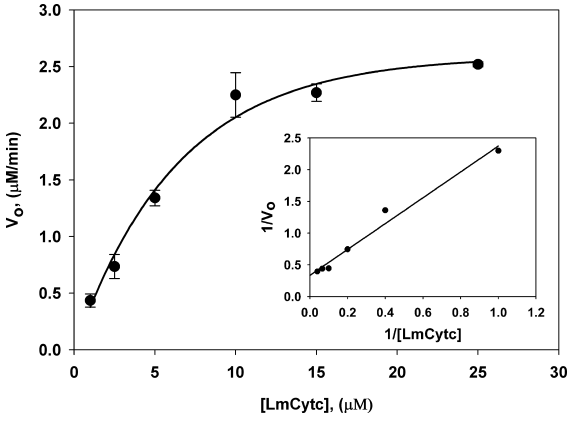

Figure 4. Michealis–Menten curve of LmP oxidation of LmCytc. K_M and k_{cat} used to determine efficiency (k_{cat}/K_M) were calculated using the equation obtained from the Lineweaver–Burk plot (inset). The reaction mixtures included 25 mM potassium phosphate (pH 6.5), 50 pM LmP, and 0.180 mM hydrogen peroxide.

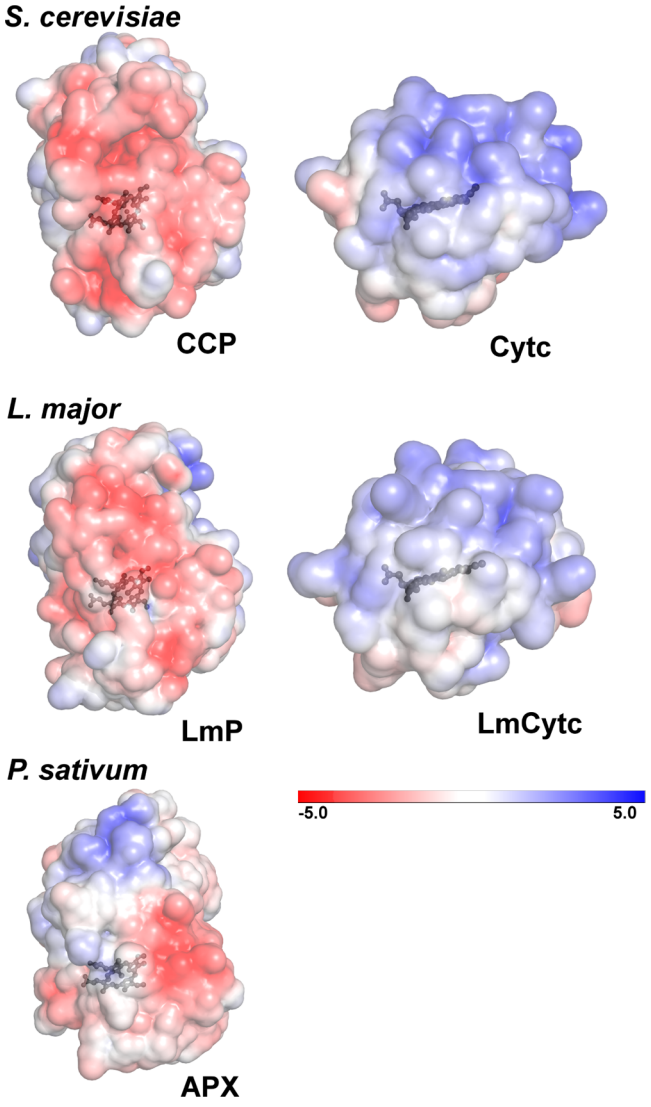

Figure 5. Electrostatic surface representations (±5kT) of *S. cerevisiae* CCP and Cytc, *L. major* LmP and LmCytc, and, as a control, cytosolic pea ascorbate peroxidase (APX). These surfaces are the same ones that would be involved in substrate binding as determined by the cocrystal structure of the *S. cerevisiae* system (PDB entry 2PCC). Both *S. cerevisiae* and *L. major* heme peroxidases have an overall distribution of negative charge at the Cytc binding interface, while the respective Cytc substrates have a clearly positive distribution. *Pisum sativum* APX does not have a strong distribution of negative charge on the same surface. These figures were generated with the Adaptive Poisson–Boltzmann Solver (APBS) plug-in using PyMOL.[34]

dx.doi.org/10.1021/bi300169x | *Biochemistry* 2012, 51, 2453–2460

adjustments will not relieve these clashes, although minor translations of LmCytc over the surface of LmP will relieve close contacts. To obtain a more objective model of the complex, we employed computer docking as implemented in the Rosetta package of programs.[31−33]

We began by using the yeast CCP system as a control that also was used by Gray et al. in testing Rosetta.[32] One approach in using Rosetta is to optimize side chain torsion angles on the individual redox partners first, which is called prepacking. The docking run then is initiated starting with the CCP−Cytc complex as observed in the crystal structure. The docking run is either global where the entire surface of CCP is sampled by Cytc or local refinement where Cytc is allowed only small perturbations from the initial complex. Docking results for which there is a high level of confidence from Rosetta are typically identified at the bottom of a characteristic "funnel" obtained by plotting the rmsd from the starting complex versus an energy score of the resulting structures. As shown in Figure 6, reasonable funnels are obtained for local searches but not

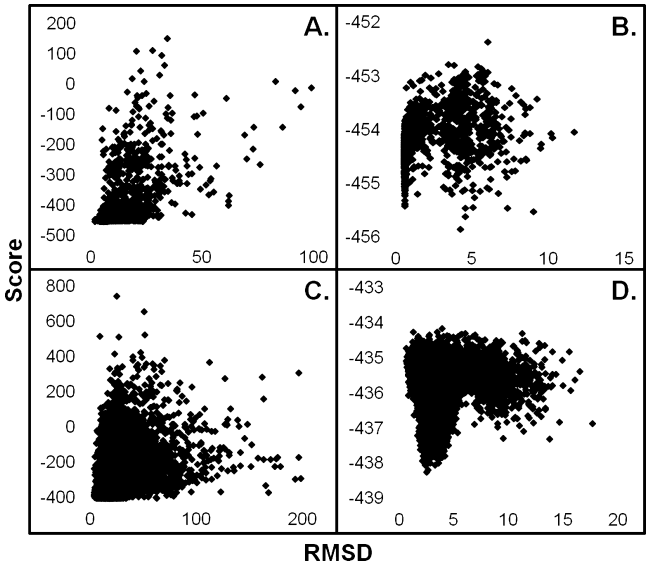

Figure 6. Rosetta docking results of rmsd vs score for the *S. cerevisiae* (PDB entry 2PCC) and *L. major* systems. Global searches for the yeast (A) and the Lm (C) system exhibit similar trends. The local refinement of the yeast system (B) illustrates a pseudofunnel. The presence of a high-confidence funnel is visible in the local refinement search of LmP (D).

global. In other systems, good funnels are observed where the correct docked complex is unique and tight as in antibody−antigen interactions. Electron transfer complexes like the CCP−Cytc complex, however, are not in this class of "hand-in-glove" fit but can be considered as two oppositely charged surfaces forming a complex where the differences in interaction energy between the electron transfer active complex and other less productive complexes are small. In other words, such complexes are "dynamic", as evidenced by recent NMR studies.[34] Therefore, it is not too surprising that the funnel is not very well-defined for a global search while the funnel is better defined during the local refinement searches, when the Cytc is restricted to sample the surface within the starting model. The best (lowest-energy) Rosetta model exhibits an rmsd of 4.2 Å from the starting structure. Figure 7 shows the Rosetta model superimposed on the crystal structure. A close examination of the structures suggests that in the Rosetta model Cytc rotates from its starting position to allow Lys79 in Cytc to form more optimal interactions with CCP but in the crystal structure Lys79 does not interact with CCP at all. In the crystal structure, ordered solvent is situated between CCP and Cytc, and this is not taken into account in Rosetta; therefore, direct interprotein electrostatic interactions dominate in Rosetta. Even so, the Rosetta model is a close approximation to the crystal structure, and the 4.2 Å rmsd from the starting crystal structure provides an estimate of error for docking of LmCytc to LmP.

The lowest-energy Rosetta model for the LmP−LmCytc local docking using the same prepacking protocol used for the yeast system exhibits an rmsd of only 2.5 Å from the starting model (Figure 7) and indicates that the LmP−LmCytc complex is very similar to the yeast complex. The Rosetta model also predicts some distinct differences between the yeast and Lm redox pairs. In the LmP−LmCytc complex, Lys83 of LmCytc is ∼4 Å from Asp216 in LmP. The residue corresponding to Asp216 in yeast CCP is Thr199, so the Lm system has the potential to make at least one strong interprotein ion pairing not possible in the yeast system. It also should be noted that Asp216 is within 3.9 Å of the K^+ ion in LmP. A monovalent cation is also found at this position in APX and is Ca^{2+} in many other peroxidases, while yeast CCP has water at this location rather than a cation.

We ran one additional control using horse heart Cytc. It is well-known that, compared to yeast Cytc, horse heart Cytc is a poorer substrate for yeast CCP.[30] In addition, the crystal structure of the yeast CCP−horse heart Cytc complex also exhibits subtle but distinct differences from the CCP−yeast Cytc complex.[28] Rosetta docking using horse heart Cytc (data not shown) shows no well-defined funnel for either global or local docking. Thus, the nonphysiological complex gives the poorest docking results.

Conclusions. In this study, we have shown that LmCytc is a much better substrate for LmP than horse heart Cytc and that the activity approaches that of yeast CCP. Given the location of LmP in the mitochondria[13] and a much higher level of activity toward LmCytc, we conclude that the biological function of LmP is to oxidize LmCytc. The crystal structure of LmCytc has allowed us to develop a model of the LmP−LmCytc complex using the yeast system as a guide. The computer docked model is very close to the yeast CCP−Cytc crystal structure, although there are some distinct differences. The crystal structure shows that there are no direct ion pairs in the yeast CCP−Cytc complex, but Rosetta attempts to optimize ion pairing by rotating Cytc in such a way as to allow Lys79 to come within 4.1 Å of Glu201 in CCP. This movement of Cytc requires disruption of nonbonded contacts involving Ala194 and Val197 in CCP with Ala81 in Cytc. It thus appears that Rosetta favored charge−charge interactions at the expense of nonpolar interactions. LmP cannot form the same nonpolar interactions as in CCP. The residues corresponding to CCP Ala194 and Val197 in LmP are Asp211 and Gly241, respectively, so nonpolar interactions may be less important in the LmP−LmCytc complex. Moreover, the LmP−LmCytc complex can form one ion pair not possible in the yeast redox partners. These differences correlate well with differences in ionic strength dependence. In yeast CCP, activity increases with an increasing ionic strength, which will promote nonpolar interactions. As the ionic strength increases above 100 mM, activity decreases because of electrostatic masking. Thus, the

dx.doi.org/10.1021/bi300169x | *Biochemistry* 2012, 51, 2453−2460

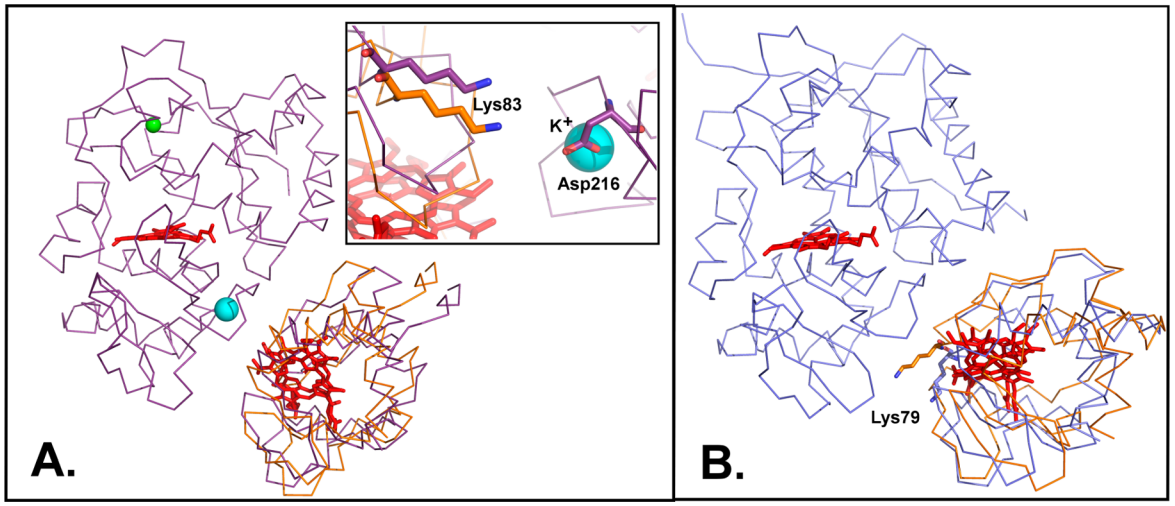

Figure 7. Input and output structures from Rosetta docking. (A) The LmP prepacked input structure is colored purple. The lowest-rmsd output of LmCytc is colored orange. Rosetta optimized ionic interactions, such as those of Asp216 and Lys83 (inset). The large cyan sphere is a potassium ion bound in LmP, which is not present in yeast CCP. (B) CCP and Cytc cocrystal coordinates (PDB entry 2PCC); the input structure is colored blue. The lowest-rmsd output of cytc is colored orange. Lys79 is shifted to more favorably interact with CCP.

yeast CCP system is a balance between nonpolar and electrostatic interactions. However, the LmP−LmCytc system exhibits a steady decrease in activity with an increasing ionic strength, suggesting that nonpolar interactions are less important and that electrostatic interactions dominate. As noted, these experimental differences correlate well with distinct differences at the docking interfaces, adding a level of confidence that our model of the LmP−LmCytc complex is a very good approximation of the physiologically relevant complex.

■ ASSOCIATED CONTENT

Accession Codes

The coordinates of *L. major* cytochrome *c* have been deposited in the Protein Data Bank as entry 4DY9.

■ AUTHOR INFORMATION

Corresponding Author

*E-mail: poulos@uci.edu. Phone: (949) 824-7020.

Funding

This work was supported by National Institutes of Health Grant GM42614.

Notes

The authors declare no competing financial interest.

■ ACKNOWLEDGMENTS

We thank Dr. Yergalem T. Meharenna for designing and ordering the LmCytc expression construct from GenScript and Taylor R. Page (Northwestern University, Evanston, IL) for his streamlined Cytc expression and purification protocols that expedited purification of LmCytc. We also thank Prof. Grant A. Mauk (University of British Columbia, Vancouver, BC) for the pBTR1 yeast iso-1-cytochrome *c* expression system.

■ ABBREVIATIONS

rmsd, root-square-mean deviation; LmP, *L. major* peroxidase; LmCytc, *L. major* cytochrome *c*; CCP, *S. cerevisiae* cytochrome *c* peroxidase; Cytc, cytochrome *c*; LB, Luria broth; TB, Terrific broth; CV, column volume; R_z, Reinheits Zahl.

■ REFERENCES

(1) Volkov, A. N., Nicholls, P., and Worrall, J. A. (2011) The complex of cytochrome c and cytochrome c peroxidase: The end of the road? *Biochim. Biophys. Acta 1807*, 1482−1503.

(2) Dolphin, D., Forman, A., Borg, D. C., Fajer, J., and Felton, R. H. (1971) Compounds I of catalase and horse radish peroxidase: π-cation radicals. *Proc. Natl. Acad. Sci. U.S.A. 68*, 614−618.

(3) Sivaraja, M., Goodin, D. B., Smith, M., and Hoffman, B. M. (1989) Identification by ENDOR of Trp191 as the free-radical site in cytochrome c peroxidase compound ES. *Science 245*, 738−740.

(4) Adak, S., and Datta, A. K. (2005) *Leishmania major* encodes an unusual peroxidase that is a close homologue of plant ascorbate peroxidase: A novel role of the transmembrane domain. *Biochem. J. 390*, 465−474.

(5) Dolai, S., Yadav, R. K., Datta, A. K., and Adak, S. (2007) Effect of thiocyanate on the peroxidase and pseudocatalase activities of *Leishmania major* ascorbate peroxidase. *Biochim. Biophys. Acta 1770*, 247−256.

(6) Yadav, R. K., Dolai, S., Pal, S., and Adak, S. (2008) Role of tryptophan-208 residue in cytochrome c oxidation by ascorbate peroxidase from *Leishmania major*: Kinetic studies on Trp208Phe mutant and wild type enzyme. *Biochim. Biophys. Acta 1784*, 863−871.

(7) Barrows, T. P., Bhaskar, B., and Poulos, T. L. (2004) Electrostatic control of the tryptophan radical in cytochrome c peroxidase. *Biochemistry 43*, 8826−8834.

(8) Bhaskar, B., Bonagura, C. A., Li, H., and Poulos, T. L. (2002) Cation-induced stabilization of the engineered cation-binding loop in cytochrome c peroxidase (CcP). *Biochemistry 41*, 2684−2693.

(9) Bonagura, C. A., Bhaskar, B., Sundaramoorthy, M., and Poulos, T. L. (1999) Conversion of an engineered potassium-binding site into a calcium-selective site in cytochrome c peroxidase. *J. Biol. Chem. 274*, 37827−37833.

(10) Bonagura, C. A., Sundaramoorthy, M., Bhaskar, B., and Poulos, T. L. (1999) The effects of an engineered cation site on the structure, activity, and EPR properties of cytochrome c peroxidase. *Biochemistry 38*, 5528−5545.

(11) Bonagura, C. A., Sundaramoorthy, M., Pappa, H. S., Patterson, W. R., and Poulos, T. L. (1996) An engineered cation site in cytochrome c peroxidase alters the reactivity of the redox active tryptophan. *Biochemistry 35*, 6107−6115.

(12) Jasion, V. S., Polanco, J. A., Meharenna, Y. T., Li, H., and Poulos, T. L. (2011) Crystal structure of *Leishmania major* peroxidase and characterization of the compound I tryptophan radical. *J. Biol. Chem. 286*, 24608−24615.

(13) Dolai, S., Yadav, R. K., Pal, S., and Adak, S. (2008) *Leishmania major* ascorbate peroxidase overexpression protects cells against reactive oxygen species-mediated cardiolipin oxidation. *Free Radical Biol. Med. 45*, 1520−1529.
(14) Ivens, A. C., Peacock, C. S., Worthey, E. A., Murphy, L., Aggarwal, G., Berriman, M., Sisk, E., Rajandream, M. A., Adlem, E., Aert, R., Anupama, A., Apostolou, Z., Attipoe, P., Bason, N., Bauser, C., Beck, A., Beverley, S. M., Bianchettin, G., Borzym, K., Bothe, G., Bruschi, C. V., Collins, M., Cadag, E., Ciarloni, L., Clayton, C., Coulson, R. M., Cronin, A., Cruz, A. K., Davies, R. M., De Gaudenzi, J., Dobson, D. E., Duesterhoeft, A., Fazelina, G., Fosker, N., Frasch, A. C., Fraser, A., Fuchs, M., Gabel, C., Goble, A., Goffeau, A., Harris, D., Hertz-Fowler, C., Hilbert, H., Horn, D., Huang, Y., Klages, S., Knights, A., Kube, M., Larke, N., Litvin, L., Lord, A., Louie, T., Marra, M., Masuy, D., Matthews, K., Michaeli, S., Mottram, J. C., Muller-Auer, S., Munden, H., Nelson, S., Norbertczak, H., Oliver, K., O'Neil, S., Pentony, M., Pohl, T. M., Price, C., Purnelle, B., Quail, M. A., Rabbinowitsch, E., Reinhardt, R., Rieger, M., Rinta, J., Robben, J., Robertson, L., Ruiz, J. C., Rutter, S., Saunders, D., Schafer, M., Schein, J., Schwartz, D. C., Seeger, K., Seyler, A., Sharp, S., Shin, H., Sivam, D., Squares, R., Squares, S., Tosato, V., Vogt, C., Volckaert, G., Wambutt, R., Warren, T., Wedler, H., Woodward, J., Zhou, S., Zimmermann, W., Smith, D. F., Blackwell, J. M., Stuart, K. D., Barrell, B., et al. (2005) The genome of the kinetoplastid parasite, *Leishmania major*. *Science 309*, 436−442.
(15) Pollock, W. B., Rosell, F. I., Twitchett, M. B., Dumont, M. E., and Mauk, A. G. (1998) Bacterial expression of a mitochondrial cytochrome c. Trimethylation of Lys72 in yeast iso-1-cytochrome c and the alkaline conformational transition. *Biochemistry 37*, 6124−6131.
(16) Berry, E. A., and Trumpower, B. L. (1987) Simultaneous determination of hemes a, b, and c from pyridine hemochrome spectra. *Anal. Biochem. 161*, 1−15.
(17) Dus, K., de Klerk, H., Bartsch, R. G., Horio, T., and Kamen, M. D. (1967) On the Monoheme Nature of Cytochrome c′ (*Rhodopseudomonas palustris*). *Proc. Natl. Acad. Sci. U.S.A. 57*, 367−370.
(18) Yonetani, T. (1965) Studies on cytochrome c peroxidase. II. Stoichiometry between enzyme, H_2O_2, and ferrocytochrome c and enzymic determination of extinction coefficients of cytochrome c. *J. Biol. Chem. 240*, 4509−4514.
(19) Fowler, R. M., and Bright, H. A. (1935) Standardization of permanganate solutions with sodium oxalate. *J. Res. Natl. Inst. Stand. Technol. 15*, 493−575.
(20) Otwinowski, Z., and Minor, W. (1997) Processing of X-ray diffraction data collected in oscillation mode. *Methods Enzymol. 276*, 307−326.
(21) McCoy, A. J. (2007) Solving structures of protein complexes by molecular replacement with Phaser. *Acta Crystallogr. D63*, 32−41.
(22) Winn, M. D., Ballard, C. C., Cowtan, K. D., Dodson, E. J., Emsley, P., Evans, P. R., Keegan, R. M., Krissinel, E. B., Leslie, A. G., McCoy, A., McNicholas, S. J., Murshudov, G. N., Pannu, N. S., Potterton, E. A., Powell, H. R., Read, R. J., Vagin, A., and Wilson, K. S. (2011) Overview of the CCP4 suite and current developments. *Acta Crystallogr. D67*, 235−242.
(23) Potterton, L., McNicholas, S., Krissinel, E., Gruber, J., Cowtan, K., Emsley, P., Murshudov, G. N., Cohen, S., Perrakis, A., and Noble, M. (2004) Developments in the CCP4 molecular-graphics project. *Acta Crystallogr. D60*, 2288−2294.
(24) Emsley, P., and Cowtan, K. (2004) Coot: Model-building tools for molecular graphics. *Acta Crystallogr. D60*, 2126−2132.
(25) Emsley, P., Lohkamp, B., Scott, W. G., and Cowtan, K. (2010) Features and development of Coot. *Acta Crystallogr. D66*, 486−501.
(26) Adams, P. D., Grosse-Kunstleve, R. W., Hung, L. W., Ioerger, T. R., McCoy, A. J., Moriarty, N. W., Read, R. J., Sacchettini, J. C., Sauter, N. K., and Terwilliger, T. C. (2002) PHENIX: Building new software for automated crystallographic structure determination. *Acta Crystallogr. D58*, 1948−1954.
(27) Afonine, P. V., Grosse-Kunstleve, R. W., and Adams, P. D. (2005) A robust bulk-solvent correction and anisotropic scaling procedure. *Acta Crystallogr. D61*, 850−855.
(28) Pelletier, H., and Kraut, J. (1992) Crystal structure of a complex between electron transfer partners, cytochrome c peroxidase and cytochrome c. *Science 258*, 1748−1755.
(29) Bushnell, G. W., Louie, G. V., and Brayer, G. D. (1990) High-resolution three-dimensional structure of horse heart cytochrome c. *J. Mol. Biol. 214*, 585−595.
(30) Kang, C. H., Ferguson-Miller, S., and Margoliash, E. (1977) Steady state kinetics and binding of eukaryotic cytochromes c with yeast cytochrome c peroxidase. *J. Biol. Chem. 252*, 919−926.
(31) Chaudhury, S., Berrondo, M., Weitzner, B. D., Muthu, P., Bergman, H., and Gray, J. J. (2011) Benchmarking and analysis of protein docking performance in Rosetta v3.2. *PLoS One 6*, e22477.
(32) Gray, J. J., Moughon, S., Wang, C., Schueler-Furman, O., Kuhlman, B., Rohl, C. A., and Baker, D. (2003) Protein-protein docking with simultaneous optimization of rigid-body displacement and side-chain conformations. *J. Mol. Biol. 331*, 281−299.
(33) Wang, C., Bradley, P., and Baker, D. (2007) Protein-protein docking with backbone flexibility. *J. Mol. Biol. 373*, 503−519.
(34) Bashir, Q., Volkov, A. N., Ullmann, G. M., and Ubbink, M. (2010) Visualization of the encounter ensemble of the transient electron transfer complex of cytochrome c and cytochrome c peroxidase. *J. Am. Chem. Soc. 132*, 241−247.